AD_____

GRANT NUMBER DAMD17-96-1-6129

TITLE: Metastatic Tumor Cell Behavior In Situ

PRINCIPAL INVESTIGATOR: John Condeelis, Ph.D.

CONTRACTING ORGANIZATION: Albert Einstein College of Medicine
Bronx, New York 10461

REPORT DATE: October 1997

TYPE OF REPORT: Annual

PREPARED FOR: Commander
U.S. Army Medical Research and Materiel Command
Fort Detrick, Maryland 21702-5012

REPORT DOCUMENTATION PAGE

Form Approved
OMB No. 0704-0188

1. AGENCY USE ONLY *(Leave blank)*	2. REPORT DATE	3. REPORT TYPE AND DATES COVERED
	October 1997	Annual (15 Sep 96 - 14 Sep 97)

4. TITLE AND SUBTITLE
Metastatic Tumor Cell Behavior in Situ

5. FUNDING NUMBERS
DAMD17-96-1-6129

6. AUTHOR(S)
John Condeelis, Ph.D.

7. PERFORMING ORGANIZATION NAME(S) AND ADDRESS(ES)
Albert Einstein College of Medicine
Bronx, NY 10461

8. PERFORMING ORGANIZATION REPORT NUMBER

9. SPONSORING/MONITORING AGENCY NAME(S) AND ADDRESS(ES)
Commander
U.S. Army Medical Research and Materiel Command
Fort Detrick, Frederick, Maryland 21702-5012

10. SPONSORING/MONITORING AGENCY REPORT NUMBER

11. SUPPLEMENTARY NOTES

12a. DISTRIBUTION / AVAILABILITY STATEMENT
Approved for public release; distribution unlimited

12b. DISTRIBUTION CODE

13. ABSTRACT *(Maximum 200*

Metastasis is the leading cause of the death in cancer patients. Cell motility is believed to be a necessary step in the metastatic process[1]. Currently, most methods available to study the behavior of metastatic tumor cells are indirect, e.g., cell motility is examined *in vitro* and the results are correlated with metastatic capability[2]. We have developed a model that directly examines the motility of metastatic primary tumor cells *in situ*. A metastatic rat breast cancer cell line was established that constitutively expresses the green fluorescent protein (GFP). Upon subcutaneous injection of these cells into the mammary fat pad of female Fischer 344 rats, primary tumors and subsequent metastases form that fluoresce when excited with light passed through an FITC filter set. Animations of metastatic tumor cells moving in live rats were generated by intravital imaging of the primary tumor, *in situ*, on a laser scanning confocal microscope. With this model, the behavioral phenotype of tumor cells can be described and the effects of genetic manipulations or therapeutic treatments on this phenotype can be determined[3]. This is the first report of visualization of cells in a primary tumor in live animals in a clinically relevant model.

14. SUBJECT TERMS Breast Cancer	15. NUMBER OF PAGES 18
	16. PRICE CODE

17. SECURITY CLASSIFICATION OF REPORT	18. SECURITY CLASSIFICATION OF THIS PAGE	19. SECURITY CLASSIFICATION OF ABSTRACT	20. LIMITATION OF ABSTRACT
Unclassified	Unclassified	Unclassified	Unlimited

FOREWORD

Opinions, interpretations, conclusions and recommendations are those of the author and are not necessarily endorsed by the U.S. Army.

✓ Where copyrighted material is quoted, permission has been obtained to use such material.

✓ Where material from documents designated for limited distribution is quoted, permission has been obtained to use the material.

✓ Citations of commercial organizations and trade names in this report do not constitute an official Department of Army endorsement or approval of the products or services of these organizations.

✓ In conducting research using animals, the investigator(s) adhered to the "Guide for the Care and Use of Laboratory Animals," prepared by the Committee on Care and Use of Laboratory Animals of the Institute of Laboratory Resources, National Research Council (NIH Publication No. 86-23, Revised 1985).

___ For the protection of human subjects, the investigator(s) adhered to policies of applicable Federal Law 45 CFR 46.

✓ In conducting research utilizing recombinant DNA technology, the investigator(s) adhered to current guidelines promulgated by the National Institutes of Health.

✓ In the conduct of research utilizing recombinant DNA, the investigator(s) adhered to the NIH Guidelines for Research Involving Recombinant DNA Molecules.

✓ In the conduct of research involving hazardous organisms, the investigator(s) adhered to the CDC-NIH Guide for Biosafety in Microbiological and Biomedical Laboratories.

PI - Signature 10/1/97 Date

Table of Contents:

Introduction:

To date, models used to perform intravital imaging of metastatic cells have been artificial in nature, such as heterologous systems and systemic injection of cells, or have provided a low resolution that does not permit observations at the cellular level [4,5]. Alternatively, studies that visualize orthotopically transplanted tumors do not allow observations of cellular activity because the tissue is dissected out prior to viewing[6]. We describe a spontaneous model of metastasis in which a live animal was used to examine, at high resolution, the surface activity and motility of metastatic primary tumors growing orthotopically in immune competent rats.

The highly metastatic MTLn3 cell line, derived from the chemically induced 13762NF rat mammary adenocarcinoma, was co-transfected with the pGreenLantern-1 vector (Gibco), which contains the cDNA for a humanized S65T mutant of GFP, and the pSV7neo vector. One clone, MTLn3+GFP, was chosen for its ability to retain both a fluorescent phenotype and resistance to neomycin in culture. The growth rate and morphology of the MTLn3+GFP cells does not deviate from that of parental MTLn3 cells. The transfected cells appear uniformly fluorescent and the cell perimeters are easily defined. The fluorescence level of the MTLn3+GFP cells remains stable through thirty passages in culture. This was verified by measuring the fluorescence intensity of

MTLn3+GFP cell lysates, at various culture passage numbers, on a fluorescence spectrophotometer.

The metastatic involvement of tissues from rats injected with MTLn3 cells was summarized previously in Neri et al. and Edmonds et al.[7,8]. The pattern of involvement seen in this model is closely correlated with what is seen clinically in breast cancer patients[9]. To establish that, at varying time points after inoculation, MTLn3+GFP cells would form primary tumors and metastases to the same extent, and with the same time scale as the parental MTLn3 cells; an extensive histopathological examination of the pattern of metastatic tissue involvement of the MTLn3+GFP cells was performed. The results of this study indicate that the MTLn3+GFP cells retain the same metastatic phenotype displayed by the parental MTLn3 cells (Farina, K., Wyckoff, J., Segall, J., Condeelis, J., Jones, J., in preparation, 1997).

Body:

Primary tumors and tissues with secondary involvement were dissected and viewed with light passed through an FITC filter set. We found that the primary tumor was brightly fluorescent (Fig 1A). Primary tumors and their blood vessels are easily identifiable; the tumors themselves appear much brighter than the background of host tissue. This fluorescence could also be seen in metastatic tumors of the lymph nodes (data not shown) and lungs (Fig 1B). The fluorescent phenotype of the MTLn3+GFP cells persisted in primary tumors and metastases throughout the life span of the animals injected. Based on these results we analyzed the motility of fluorescent MTLn3 cells in primary tumors growing in live animals.

All intravital imaging (Fig 2) was carried out on the laser scanning confocal microscope (Bio-Rad MRC 600). In images of regions containing both primary tumor and blood vessels, the blood vessels appear black. Single tumor cells bordering a blood vessel could be identified in the tumor shown in figure 3. This is an image of an intact primary tumor in a live animal. The observation of blood flowing freely in the tumor's vasculature indicated that the blood supply to the tissue was not disrupted; therefore the tissue was healthy and functional during viewing.

In order to determine the characteristics of cell motility *in vivo*, the tumor shown in figure 3 was imaged at high resolution at 2 minute intervals. Fig 4 shows a single cell of figure 3B as a series of difference pictures, rendered from

DIAS software, which demonstrates the random motility of the cell. It is apparent from this series of images that cell perimeters are easily defined with this technology. This allows identification of changes in cell shape, including extensions and retractions of pseudopods, observations which are crucial to descriptions of cell motility. Figure 4B consists of three still frames obtained by imaging an intact primary tumor in a live animal at two mintue intervals. The directed protrusion of the marked cell is clearly demonstrated as it makes its way into the field of view over a six minute time period. A series of DIAS difference pictures from t = 10 - 16 min. is shown in figure 4C. In this figure, the arrows that represent the direction of cell centroid translocation show successive cell movements in the same general direction. This is distinct from the type of cell movement seen in figure 4A, where the cell remains stationary while it extends and retracts pseudopods in all directions.

Photobleaching of fluorophores is a common drawback of laser scanning confocal microscopy; it can lead to dramatic misinterpretation of results. In our model system, a thirty percent decrease in pixel intensity was calculated over the course of one hour. This did not affect our analyses since this level of photobleaching did not prevent identification of cell margins.

Cellular locomotion was observed repeatedly in several experiments. However, in all of the tumors examined, it was apparent that only a small fraction of tumor cells are actively motile. One of these motile cells is shown, in figure 5A, as it moves across the field. Fig 5B demonstrates some types of analyses that

can be performed to describe cell motility and behavior. Centroid and perimeter plots are shown of the cell tracked by the arrow in 5A. From these plots, an instantaneous velocity of 3.4 +/- 1.5 μm/min. Although we have not set out to describe a behavioral phenotype in this report, these values are included to demonstrate the types of parameters that can be determined with this model. Additional parameters that one can compute using a DIAS analysis are described elsewhere[3].

Through the use of this model, we have observed locomotion of metastatic primary tumor cells and surface features of these movements in live animals. It is clear that these tumor cells are actively motile as they disseminate from their primary site. This information supports the three step hypothesis of metastasis[1] which purports that motility is necessary for a cell to metastasize. This model will be useful not only in describing and tracking the behavior and interactions of these metastatic tumor cells *in vivo*, but also in assessing the effects that genetic manipulations of key cytoskeletal proteins impart on cell motility and metastasis[10,11,12,13]. It will provide a means to evaluate the impacts of treatment modalities such as pharmaceuticals, radiation, and chemotherapy on metastatic tumor cell behavior *in vivo*. It is the first model that allows direct observations of metastasis in an intact orthotopically grown primary tumor while in a live animal.

Conclusions:

We expect that further modifications can improve the resolution of this model. Increased intensity of fluorescence can be achieved by transfection of tumor cells with new genetically enhanced versions of GFP that have increased emission and expression[14,15,16]. We have already successfully acquired z-series during time lapse imaging to generate three dimensional views of cell movement (data not shown). New confocal technology with more sensitive detectors and higher speeds of image acquisition will significantly increase the spatial and temporal resolution of this type of cell imaging in intact tissue.

References

1. Steller-Stevenson, W.G., Aznovoorian, S., and Liotta, L.A. Tumor cell interactions with the extracellular matrix during invasion and metastasis. *Ann. Rev. Cell. Bio.* **9,** 541-573 (1993).

2. Partin, A.W, Mohler, J.L., and Coffey, D.S. Cell motility as an index of metastatic ability in prostate cancers. *Cancer Treat. Res.* **59,** 121-130 (1992).

3. Soll, D.R. The use of computers in understanding how animal cells crawl. *Int. Rev. Cytology.* **163,** 43-104 (1995).

4. MacDonald, I.C. *et al.* Intravital videomicroscopy of the chorioallantoic microcirculation. *Microvascular Research.* **44,** 185-199 (1992).

5. Morris, V.L *et al.* Early interactions of cancer cells with the microvasculature in mouse liver and muscle during hematogenous metastasis; videomicroscopic analysis. *Clin. Exp. Metastasis.* **11,** 377-390 (1993).

6. Chishima, T. *et al.* Cancer invasion and micrometastasis visualized in live tissue by green fluorescent protein expression. *Cancer Research.* **57,** 2042-2047 (1997).

7. Neri, A. *et al.* Development and biologic properties of malignant cell sublines and clones of a spontaneously metastasizing rat mammary adenocarcinoma. *Journal of NCI.* **68,** 507-517 (1982).

8. Edmonds, B. *et al.* Elongation factor-1α is an overexpressed actin binding protein in metastatic rat mammary adenocarcinoma. *J. Cell Science.* **109,** 2705-2714 (1996).

9. Haagensen, C.D. The natural history of breast cancer in *Diseases of the Breast. 3rd ed.* 635-718. Philadelphia, W.B. Saunders Co.,. (1986).

10. Cunningham, C.C., Gorlin, J.B., Kwiatkowski, D.J., Hartwig, J.H., Janmey, P.A., Byers, H.R., and Stossel, T.P. Actin-binding protein requirement for cortical stability and efficient locomotion. *Science.* **255,** 325-327 (1992).

11. Cox, D., Condeelis, J., Wessels, D., Soll, D.R., Kern, H., and Knecht, D.A. Targetted disruption of the ABP-120 gene leads to cells with altered motility. *J. Cell Biol.* **116,** 943-955 (1992).

12. Wessels, D., Soll, D.R., Knecht, D., Loomis, W.F., DeLozanne, A., and Spudich, J. Cell motility and chemotaxis in *Dictyostelium* amoebae lacking myosin heavy chain. *Dev. Biol.* **128,** 164-177 (1988).

13. Wessels, D., Murray, J., Jung, G., Hammer, J.A., III, and Soll, D.R. Myosin 1B null mutants of *Dictyostelium* exhibit abnormalities in movement. *Cell Motil. Cytoskel.* **20,** 301-315 (1990).

14. Yang, T-T., Cheng, L., Kain, S.R. Optimized codon usage and chromophore mutations provide enhanced sensitivity with the green fluorescent protein. *Nuc. Acids Rsch.* **22,** 4592-4593 (1996).

15. Zhang, G., Gurtu, V., and Kain, S.R. An enhanced green fluorescent protein allows sensitive detection of gene transfer in mammalian cells. *Bioch. and Biophys. Comm.* **227,** 707-711 (1996).

16. Kimata, Y., Iwaki, M., Lim, C.R., and Kohno, K. A novel mutation which enhances the fluorescence of green fluorescent protein at high temperatures. *Bioch. and Biophys. Comm.* **232,** 69-73 (1997).

17. Petry, J.J. The anatomy of the epigastric flap in the experimental rat. *Plastic and Reconstructive Surgery.* **74,** 410-413 (1984).

18. Mutaf, M. The rat saphenous flap: A fasciocutaneous free flap model without panniculus carnosus. *Annals of Plastic Surgery.* **35,** 402-408 (1995).

19. Maron, M.J. *Numerical Analysis*. New York, Macmillan Publishing Co., (1982).

Appendices:

Figure 1 (dissected PT and lungs)

A. Brightly fluorescent MTLn3+GFP cell induced primary tumor viewed on a Zeiss Axiophot microscope at 1.5X magnification. This tumor was dissected two weeks after injection of 1.5 X 10^6 cells into the mammary fat pad. For viewing this and other dissected tissues, animals were sacrificed in a CO_2 chamber. All dissected tissue was kept alive by maintenance in ice cold PBS and viewed immediately. **B.** Projection of lung metastasis in lung dissected four weeks after injection. This image was taken on the Bio Rad MRC 600 scanning laser confocal microscope equipped with a 20X dry objective (Nikon; Apochromat; NA = 0.5). To generate this image, consecutive focal planes were imaged using a z-axis stepping motor. The image shown is a projection of the z-series constructed by COMOS software using a maximum algorithm.

figure 2 (rat diagram)

To produce primary tumors, we adhered to the protocol described by Neri *et al.* Briefly, subcutaneous injection of MTLn3 cells into the mammary fat pad of these rats results in primary tumor formation followed by subsequent metastasis to the lymph nodes and lungs. **A.** For intravital imaging, the animals are anesthetized by isoflurane inhalation. The primary tumor is surgically exposed, creating a skin flap that allows the tumor to be viewed while maintaining an intact blood supply

from the superficial branch of the femoral artery. (a) primary tumor, (b) skin flap, (c) superficial epigastric branch of the femoral artery, (d) lateral thoracic artery [17,18]. For viewing the tumor *in vivo,* an acrylic platform with a coverslip window was designed. The platform rests on the microscope stage with the coverslip over the objective. The animal lies to the side of the coverslip window while the skin flap is extended from the animal. The tumor lies directly on the coverslip. (a) primary tumor, (b) glass coverslip, (c) plexiglass tray, (d) anesthesia mask, (e) objective. This apparatus allowed animals to be maintained in a live state for several hours, facilitating extended viewing times.

figure 3 (stereo pairs of PT)

Paired stereo projections of primary tumor cells bordering a blood vessel at **(A)** 10X and **(B)** 20X magnification. Black outlined regions represent blood vessels running through the primary tumor. All intravital imaging was carried out on a Bio Rad MRC 600 laser scanning confocal microscope attached to a Nikon Diaphot microscope. The microscope was equipped with either a 10X dry objective (Nikon....), a 20X dry objective (Nikon; Apochromat; NA = 0.5) or a 40X dry objective (Nikon; Apochromat; NA = 0.75).These projections were generated as described in figure 2 legend. Scale bars = 100 μm.

figure 4

A. Shape change and random motility as shown by a single primary tumor cell. Images were obtained from an intact primary tumor in a live animal at two minute intervals using confocal microscopy. Animations were generated using NIH Image software. Difference analysis was performed with 2D-DIAS program (Solltech, Iowa City, IA, USA). Difference pictures were generated by superimposing successive frames. Each frame displays the direction of cell centroid translocation between earlier and later images as noted by an arrow. Green represents protrusive areas, red represents retracted areas, common zones are grey. Magnification, 20X; Scale bar = 25 μm. **B.** Primary tumor cell showing protrusive activity during intravital imaging. Images were obtained at two minute intervals using confocal microscopy. Three images from the time lapse represen a six minute time period. Arrows are located at the same coordinates in each frame. Note the increased protrusion of the tumor towards the arrowhead in panel as time progresses from left to right. **C.** DIAS difference pictures showing the protrusion of the cell.....Magnification, 20X; Scale bar = 25 μm.

figure 5

A. Motile primary tumor cells. Images were obtained at two minute intervals during intravital imaging of an intact primary tumor 2.5 weeks post injection. Time lapse imaging was performed by obtaining single optical sections that were scanned eight times and Kalman averaged at each time point. The arrow follows a single cell through t=20-38 min. The arrowhead points to the stationary tumor

mass. Magnification, 20X; Scale bar, 25 μm. **B.** The path followed by the cell tracked in A presented as a cell perimeter plot and a centroid plot. Cell motility parameters were analyzed according to methods previously described. The cell perimeter was manually traced and digitized with DIAS sotware. Centroid location at each time point was computed from x, y coordinates of the pixels at the perimeter of the digitized cell image. The central difference method described by Maron[19] was used to determine instantaneous "velocity" (μm/min). Directional change was calculated as the absolute difference in centroid location between two consecutive frames.

1A.

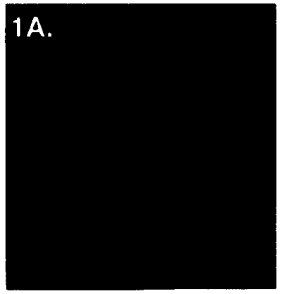

1B.

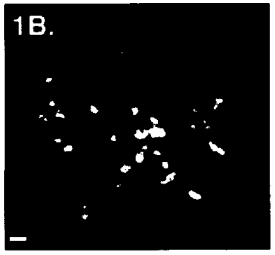

2.

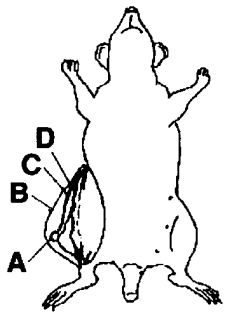

A - Primary Tumor
B - Skin Flap
C - Superficial Epigastric Branch of Femoral Artery
D - Lateral Thoracic Artery

3A.

3B.

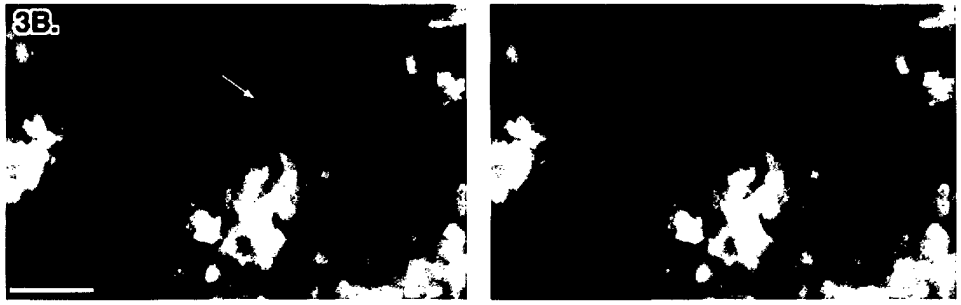

4A.

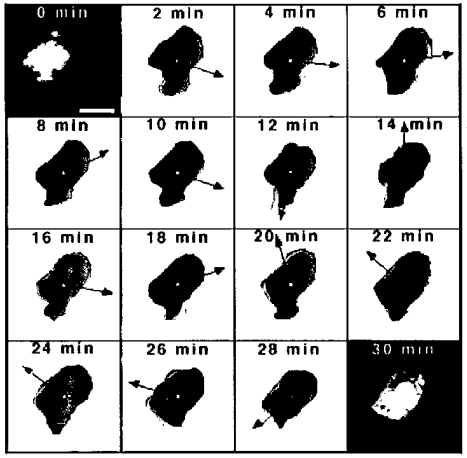

4B.

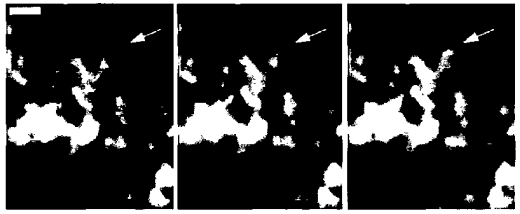

4C.

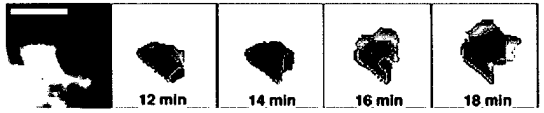

5A.

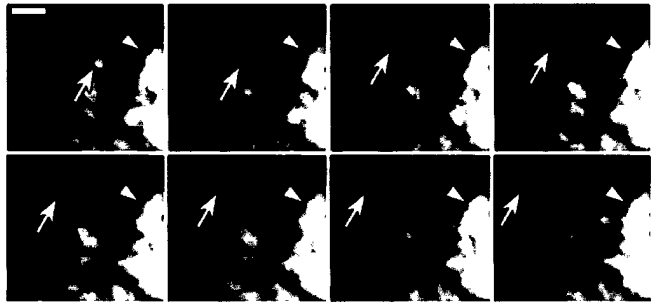

5B.